



# HHS Public Access

Author manuscript

*Nat Struct Mol Biol.* Author manuscript; available in PMC 2021 September 23.

Published in final edited form as:

*Nat Struct Mol Biol.* 2009 November ; 16(11): 1141–1147. doi:10.1038/nsmb.1682.

## Hsp90 charged-linker truncation reverses the functional consequences of weakened hydrophobic contacts in the N domain

Shinji Tsutsumi<sup>#1,7</sup>, Mehdi Mollapour<sup>#1,7</sup>, Christian Graf<sup>2</sup>, Chung-Tien Lee<sup>2</sup>, Bradley T Scroggins<sup>1</sup>, Wanping Xu<sup>1</sup>, Lenka Haslerova<sup>3</sup>, Martin Hessling<sup>4</sup>, Anna A Konstantinova<sup>1</sup>, Jane B Trepel<sup>5</sup>, Barry Panaretou<sup>3</sup>, Johannes Buchner<sup>4</sup>, Matthias P Mayer<sup>2</sup>, Chrisostomos Prodromou<sup>6</sup>, Len Neckers<sup>1</sup>

<sup>1</sup>Urologic Oncology Branch, National Cancer Institute, Bethesda, Maryland, USA.

<sup>2</sup>Center for Molecular Biology, University of Heidelberg, Heidelberg, Germany.

<sup>3</sup>Division of Life Sciences, King's College London, London, UK.

<sup>4</sup>Department of Chemistry, Technische Universität München, München, Germany.

<sup>5</sup>Medical Oncology Branch, National Cancer Institute, Bethesda, Maryland, USA.

<sup>6</sup>Section of Structural Biology, Institute of Cancer Research, Chester Beatty Laboratories, London, UK.

<sup>7</sup>These authors contributed equally to this work.

# These authors contributed equally to this work.

### Abstract

Heat shock protein 90 (Hsp90) is an essential molecular chaperone in eukaryotes, as it regulates diverse signal transduction nodes that integrate numerous environmental cues to maintain cellular homeostasis. Hsp90 also is secreted from normal and transformed cells and regulates cell motility. Here, we have identified a conserved hydrophobic motif in a  $\beta$ -strand at the boundary between the N domain and charged linker of Hsp90, whose mutation not only abrogated Hsp90 secretion but also inhibited its function. These Hsp90 mutants lacked chaperone activity *in vitro* and failed to support yeast viability. Notably, truncation of the charged linker reduced solvent accessibility of this  $\beta$ -strand and restored chaperone activity to these mutants. These data underscore the importance of  $\beta$ -strand 8 for Hsp90 function and demonstrate that the functional consequences of weakened hydrophobic contacts in this region are reversed by charged-linker truncation.

---

Correspondence should be addressed to L.N. (len@helix.nih.gov).

#### AUTHOR CONTRIBUTIONS

S.T. and M.M. performed most of the experiments and helped interpret the data, design experiments and write the manuscript; C.G., B.T.S., C.-T.L., W.X., L.H., M.H. and A.A.K. performed some of the experiments; B.P., J.B. and M.P.M. designed some of the experiments and interpreted the data collected; M.P.M. and J.B. also contributed to writing part of the manuscript; J.B.T. contributed to the design and interpretation of some of the experiments; C.P. designed and performed some of the experiments, interpreted the data collected and contributed to writing part of the manuscript; L.N. oversaw the entire project, designed experiments, interpreted the data and wrote the paper.

Supplementary information is available on the Nature Structural & Molecular Biology website.

Hsp90 is a molecular chaperone required for the stability and function of several conditionally activated, mutated or overexpressed signaling proteins that mediate cancer cell growth and survival as well as for the maintenance of normal cellular homeostasis<sup>1</sup>. Hsp90 is a conformationally flexible, modular protein that associates with distinct sets of co-chaperones depending on nucleotide occupancy of an N-terminal binding pocket. Nucleotide binding and hydrolysis drive the Hsp90 chaperone complex to bind and release client proteins.

Hsp90 is comprised of two protomers each constitutively dimerized via a well-characterized C-terminal domain, whereas transient dimerization of N-terminal domains appears to be nucleotide dependent<sup>2-4</sup>. Separating the N and C domains is the M domain, which serves as a site for client protein interaction. In eukaryotes, N and M (middle) domains are linked by an unstructured, highly charged region of divergent length and amino acid composition.

Conformational flexibility of Hsp90 is critical to its function, as Hsp90 is a ‘split’ ATPase that requires repositioning of motifs in both the N and M domains to become competent for hydrolysis<sup>2</sup>. N-terminal Hsp90 inhibitors exert their activity by interfering with these conformational changes, and they ultimately cause client proteins to be degraded by the proteasome<sup>5</sup>. Although ATP binding and hydrolysis provide directionality to the Hsp90 chaperone cycle, this process requires conformational flexibility that is inherent in nucleotide-free Hsp90 (refs. 6–11).

Although Hsp90 is highly conserved across species, the charged linker is significantly more extensive in eukaryotes than in bacteria (with the exception of the mitochondrial Hsp90 paralog TRAP1). This has been suggested to provide a gain of function to the chaperone in nucleated cells (for example, by permitting increased flexibility to accommodate an expanded repertoire of diverse client proteins and co-chaperones)<sup>8,9,12,13</sup>. However, because of its disordered nature, it has not been possible to obtain a crystal structure of the charged-linker region, making it difficult to evaluate the contribution of the charged linker to Hsp90 function. Thus, although a recent biochemical study supports a role for the charged linker in modulating nucleotide-dependent chaperone activity<sup>14</sup>, another report suggests that most of the charged linker can be removed without affecting Hsp90 function<sup>15</sup>.

Although Hsp90 is primarily an intracellular protein, its secretion to the extracellular space has been described in both normal and cancer cells, and secreted Hsp90 contributes to immune response, cell motility, wound healing and cancer metastasis<sup>16,17</sup>. Hsp90 does not have a conventional secretory signal sequence and is thought to be secreted through a nonclassical pathway, perhaps via exosomes<sup>18,19</sup>. However, the molecular determinants underlying Hsp90 secretion and any requirements for conformational flexibility in the secretory process are not known.

In this study, we have identified a highly conserved hydrophobic Ile-x-Leu (IxL) motif in a short  $\beta$ -strand ( $\beta$ -strand 8) at the boundary between the N domain and charged linker of human HSP90 $\alpha$  as a critical determinant for chaperone secretion. We demonstrate that mutation of hydrophobic residues within this motif independently affects chaperone cycling

and markedly impairs Hsp90 function *in vitro* and *in vivo*. Notably, these deleterious effects are reversed, and Hsp90 function restored, by charged-linker truncation.

## RESULTS

### N domain $\beta$ -strand 8 is a key determinant of Hsp90 secretion

In order to identify residues important for Hsp90 secretion, we mutagenized (to alanine) and screened several amino acids that available published data<sup>7,9,20,21</sup> suggested were likely to be at least partially surface exposed (Supplementary Fig. 1a). We assessed the secretory capability of the mutant proteins by transfecting COS7 cells with Flag-tagged wild-type or mutant human Hsp90 expression plasmids. Twenty-four hours after transfection, we switched the cells to serum-free medium and cultured for an additional 24 h. Conditioned medium was collected and assayed by ELISA for secreted Hsp90. One point mutation in particular, I218A, had a profound effect on Hsp90 secretion (Fig. 1a). This residue is part of a short  $\beta$ -strand ( $\beta$ -strand 8), at the junction of the N domain and charged linker, whose sequence is highly conserved (Supplementary Fig. 1b). Further investigation of this region revealed that Hsp90 secretion was also significantly impaired by L220A mutation, as well as by the double mutation I218A L220A (Fig. 1a). Notably, neither mutation of the proline residue immediately preceding the  $\beta$ -strand (Pro217) nor of the intervening threonine residue (Thr219) had a comparable impact on secretion. Intracellular expression and distribution of all mutants were equivalent to that of wild-type Hsp90 (data not shown).

### Ile218 and Leu220 are important determinants of Hsp90 function

Because the hydrophobic residues Ile218 and Leu220 are evolutionarily conserved, they are likely to affect other aspects of Hsp90 function. To address this possibility, we first determined whether these mutations affected Hsp90 interaction with client proteins. We cotransfected COS7 cells with either Flag-tagged wild-type, I218A, T219A, L220A or I218A L220A Hsp90 plasmids and with plasmid expressing the client receptor tyrosine kinase ERBB2. Immunoprecipitation with anti-Flag antibody detected ERBB2 interaction with wild-type and T219A Hsp90, but interaction with I218A and L220A mutants was slightly decreased (for quantification, see Supplementary Fig. 2a). ERBB2 interaction with the I218A L220A double mutant was greatly reduced (Fig. 1b). Similar results were obtained for two additional Hsp90 client kinases, CDK4 and RAF1 (Fig. 1b,c). Association with non-kinase clients of Hsp90, such as the glucocorticoid receptor (GR) and the androgen receptor (AR), was similarly affected by these mutations (Fig. 1d,e, and Supplementary Fig. 2).

Next, we examined the chaperone activity of Hsp90 I218A L220A *in vitro* using the Hsp90-dependent checkpoint kinase 1 (CHK1) reconstitution assay<sup>22</sup>. We incubated purified glutathione-S-transferase (GST)-CHK1 and other co-chaperone proteins with purified wild-type or I218A L220A Hsp90 protein. CHK1 kinase activity was stimulated 40-fold by wild-type Hsp90 protein, but only minimally by Hsp90 I218A L220A (Fig. 1f).

## Co-chaperone association is impacted by $\beta$ -strand 8 mutation

The Hsp90 chaperone cycle consists of an ordered series of conformationally dependent, sequential interactions with distinct co-chaperones coupled to ATP binding and hydrolysis<sup>23,24</sup>. Therefore, we tested whether co-chaperone binding was affected by mutation of Ile218 and Leu220. We transfected COS7 cells with either Flag-tagged wild-type Hsp90, I218A, T219A, L220A or I218A L220A Hsp90 mutants. Hsp90-containing protein complexes were immunoprecipitated and assessed for co-chaperone composition (for quantification, see Supplementary Fig. 2b). We detected interaction of the co-chaperone p60<sup>Hop</sup> with all Hsp90 proteins (Fig. 2a), but interaction of p60<sup>Hop</sup> with Hsp90 I218A L220A was increased, as was association of Hsp70 (Fig. 2b). In contrast, association of the co-chaperones AHA1, p23 and FKBP52 was nearly undetectable for Hsp90 I218A L220A, whereas only AHA1 interaction was noticeably reduced in the case of Hsp90 I218A (Fig. 2b,c and Supplementary Fig. 2). All Hsp90 proteins interacted efficiently with the co-chaperone p50<sup>Cdc37</sup>, and all of the Hsp90 proteins constitutively formed C-terminal dimers (Fig. 2b,d). Based on currently accepted models of the Hsp90 chaperone cycle<sup>6,10,11,20</sup>, these data suggest that mutation of the hydrophobic residues in  $\beta$ -strand 8 favors an ‘open’ conformation that is characterized by absent or reduced ATP-stabilized N-terminal dimerization and reduced affinity for client protein (Fig. 2e).

## Hsp90 $\beta$ -strand 8 mutants are lethal *in vivo*

Given the lack of *in vitro* chaperone activity of Hsp90 I218A L220A, we endeavored to examine its function *in vivo*. To accomplish this, we used a haploid *Saccharomyces cerevisiae* yeast strain (PP30 (pHSC82))<sup>25,26</sup> in which the chromosomal coding sequences of the two *S. cerevisiae* genes for Hsp90 are deleted, and viability is maintained by expression of an Hsp90 gene (*HSC82*) on the *URA3* episomal plasmid (pHSC82)<sup>26,27</sup>. Wild-type or mutant versions of Hsp90 can then be introduced on single-copy plasmids with *LEU2* as a selectable marker. The functionality of the exogenous Hsp90 protein is then examined on the basis of its ability to maintain cell viability when pHSC82 plasmid is deselected on 5-fluoroorotic acid (5-FOA)-containing plates (*URA*<sup>+</sup> cells are not viable in the presence of 5-FOA). Yeast Hsp90 residues Ile205, Gln206 and Leu207 correspond to Ile218, Thr219 and Leu220 in human HSP90 $\alpha$ . Wild-type, Q206A and L207A mutants supported yeast growth in the presence of 5-FOA, but I205A, I205A L207A and I205A Q206A L207A mutants did not (Fig. 3a). Further, although Hsp90 L207A supported yeast viability, its chaperone activity was compromised. This was shown by expressing the Hsp90 client protein v-Src in yeast. Expression of this tyrosine kinase causes lethality in yeast and is therefore a good indicator of the presence of fully functional Hsp90. In the absence of Hsp90-dependent v-Src maturation, v-Src-expressing yeast can survive, as was the case for the Hsp90 L207A mutant (Supplementary Fig. 3).

ATP binding to the N domain of Hsp90 stabilizes repositioning of an ‘ATP-lid’ loop to expose hydrophobic surfaces in each monomer whose association then generates transient N-domain dimerization<sup>24</sup>. This, in turn, creates the catalytic center of the split ATPase, promotes p23 binding to stabilize the repositioned ATP-lid and supports Aha1 binding to accelerate ATP hydrolysis<sup>2</sup>. Because we found that neither p23 nor Aha1 associates efficiently with Hsp90  $\beta$ -strand 8 mutants, we queried the nucleotide binding, N-terminal

dimerization capability and ATPase activity of these proteins (Fig. 3b; Supplementary Figs. 4 and 5). Following transfection of wild-type or I218A L220A Flag-Hsp90 proteins in COS7 cells, we examined their binding to ATP-Sepharose (Supplementary Methods), and we found that ATP binding to the I218A L220A mutant was lower than ATP binding to wild-type Hsp90 (Supplementary Fig. 5c). However, ATP binding to the Hsp90 single point mutants I218A (human) and I205A (yeast) was not significantly different from ATP binding to wild type (data not shown). Next, we used cross-linking in the presence of AMPPNP (a non-hydrolyzable analog of ATP) to show that, compared with wild-type yeast Hsp90, AMPPNP-stabilized N-terminal dimerization of the Hsp90 I205A mutant was clearly reduced (Fig. 3b; Supplementary Fig. 4). Finally, we determined the ATPase activity of these Hsp90 proteins. The ATPase activity of yeast and human Hsp90 mutants was reduced by at least 50% when compared to that of their respective wild-type controls (Fig. 3c). Notably, the ATPase activity of human Hsp90 I218A L220A was not significantly different from that of Hsp90 I218A (Fig. 3c).

Next, we determined whether reduced ATP binding and ATPase activity of these Hsp90  $\beta$ -strand 8 mutants were related causally to their impaired secretion. For this purpose, we examined the secretion of another, well-characterized nucleotide binding-impaired Hsp90 mutant (D93N) that also is considered to favor the open conformation and lacks ATPase activity<sup>26,28</sup>. Although Hsp90 D93A and I218A L220A proteins have similar defects in client protein and co-chaperone interactions, and in ATP and N-terminal inhibitor binding (Supplementary Fig. 5), secretion of Hsp90 D93A was similar to that of the wild-type protein. These data suggest that the IxL motif in  $\beta$ -strand 8 independently affects Hsp90 secretion and nucleotide-dependent chaperone cycling.

### **$\beta$ -strand 8 mutation alters Hsp90 conformational dynamics**

Our previous data suggested that the  $\beta$ -strand 8 mutation negatively affects both N-domain dimerization and ATPase activity. The rate-limiting step in the Hsp90 ATPase cycle is the ATP-induced propagation of a series of conformational changes that lead to formation of the closed state in which the N-terminal domains are transiently associated. To further explore the impact of  $\beta$ -strand 8 mutation on these events, we used fluorescence resonance energy transfer (FRET) analysis to determine the effects of the I205A mutation on specific steps of the Hsp90 conformational transition<sup>6</sup>. In agreement with our earlier data, introduction of the single point mutation I205A in yeast Hsp90 caused a clear deceleration, compared to wild-type Hsp90, of ATP $\gamma$ S-induced conformational changes. FRET efficiencies between the N domains of each protomer, and between the N domain of one protomer and the M domain of the opposing protomer, are clearly reduced in the I205A mutant when compared to wild-type Hsp90 (Fig. 4a,b).

### **Aha1-Hsp90 interaction depends on $\beta$ -strand 8**

Next, we analyzed whether Aha1 binding could induce conformational changes in Hsp90 I205A, as it does in wild-type Hsp90. As shown previously<sup>6</sup>, the addition of Aha1 to Hsp90 leads to conformational changes that rapidly bring the N domains into close proximity (Fig. 4c). However, Hsp90 I205A fails to undergo these conformational changes in the presence of Aha1, indicating either a lack of structural coupling or reduced Aha1 binding to Hsp90

I205A (Fig. 4d). We favor the latter possibility, as this would be fully consistent with our earlier observation of reduced Aha1 binding to the equivalent human Hsp90 mutant (I218A, Fig. 2b). Finally, when wild-type Hsp90 is bound to Aha1, it is more resistant to protomer dissociation, as indicated by decreased FRET between the two protomers, upon chasing the sample with unlabeled Hsp90 (ref. 6) (Fig. 4e and cartoon inset). Such Aha1-induced stabilization was not observed for Hsp90 I205A (Fig. 4f), consistent with the hypothesis that this  $\beta$ -strand 8 mutation negatively affects Aha1 binding to Hsp90.

### Charged-linker truncation restores mutant Hsp90 activity

Given these enzymatic and structural defects of  $\beta$ -strand 8 mutated Hsp90, its lack of function is not unexpected. Unlike cytosolic Hsp90, the Hsp90 paralog located in mitochondria, TRAP1, lacks an extensive charged linker separating N and M domains<sup>13</sup>. In contrast to our findings with Hsp90 I218A L220A (Supplementary Fig. 5), an equivalent mutation in TRAP1 (L285A L287A) had no impact on ATP binding (Supplementary Fig. 6). These data, and the proximity of  $\beta$ -strand 8 to the boundary between the N-domain and the adjacent charged linker in both yeast and human Hsp90, led us to speculate that the negative impact of mutating the IxL motif in  $\beta$ -strand 8 might depend on the presence of the charged linker. As deletion of most of the Hsp90 charged linker does not affect yeast viability<sup>15</sup>, we tested this hypothesis by first examining the lethality of IxL mutations in ‘linker-truncated’ ( ) yeast and human Hsp90. Notably, I205A and I205A L207A proteins were fully capable of supporting yeast viability (Fig. 5a). We obtained similar results with human I218A and I218A L220A mutants (Fig. 5b). Further, unlike the yeast Hsp90 L207A full-length mutant, the linker-truncated mutants showed robust chaperone activity when yeast were transformed with v-Src (Fig. 5c,d), and their ATPase activity was restored to that of the wild-type protein (Fig. 5e). Finally, although truncation of the charged linker itself had no effect on Hsp90 secretion, secretion of the linker-truncated human IxL  $\beta$ -strand 8 mutants was increased approximately three-fold as compared to that of their full-length counterparts (Fig. 5f).

### Hsp90 $\beta$ -strand 8 mutation alters charged-linker topology

Variation in protein sensitivity to trypsin cleavage can be used to assess different conformational states or structural alterations of proteins. Indeed, the domain structure of Hsp90 is supported by data obtained from limited proteolysis experiments<sup>29</sup>. After we transiently transfected COS7 cells with various Flag-tagged Hsp90 expression plasmids, we immunoprecipitated Hsp90 with anti-Flag antibody and, after a high salt wash to remove co-chaperones<sup>30,31</sup>, we exposed the protein to increasing concentrations of trypsin. After gel electrophoresis and protein transfer, we probed membranes with an Hsp90 antibody whose epitope is in the N terminus (amino acids 2–12)<sup>32</sup>. Wild-type Hsp90 showed the expected profile, with a predominant cleavage site in the C-terminal dimerization domain (amino acids 614/619 in human HSP90 $\alpha$ ) and a secondary cleavage site at the junction of the M domain and charged linker (amino acid 288) that became evident at higher trypsin concentrations<sup>29,32</sup> (Fig. 6a, left). Both sites in Hsp90 I218A L220A were markedly more sensitive to trypsin cleavage than the wild-type protein (Fig. 6a, right), whereas trypsin sensitivity of the site at the M domain–charged linker junction in Hsp90 I218A was clearly greater than that of the C-terminal cleavage site, which was minimally affected (Fig. 6a,

middle). These data suggest that the accessibility of the charged linker is altered in both single and double mutant proteins, but that the double mutation of Ile218 and Leu220 likely induces more global conformational changes in Hsp90 (as evidenced by increased trypsin sensitivity of the C-terminal domain). Although linker truncation nearly restores wild-type trypsin sensitivity to the C-terminal domains of both the single and double  $\beta$ -strand 8 mutant proteins, wild-type trypsin sensitivity at the charged linker–M domain junction is only partially recovered (Supplementary Fig. 7).

To further investigate the possibility that  $\beta$ -strand 8 mutation leads to altered conformation of the charged linker, we used the Hsp90 antibody K41233 (Cosmo Bio), whose epitope is within the charged-linker region and near the trypsin cleavage site at amino acid 288 (amino acids 263–270 of human HSP90 $\alpha$ <sup>29</sup>). We used K41233 in a sandwich ELISA to detect ectopically expressed, natively folded Flag-tagged Hsp90 proteins in COS7 cell extracts that had been immobilized to plates coated with anti-Flag antibody. Reactivity of the charged linker–specific antibody increased ~2.5-fold for Hsp90 I218A compared to wild-type Hsp90 and nearly 5-fold for Hsp90 I218A L220A (Fig. 6b, right). To demonstrate equal expression of the various Hsp90 proteins in COS7 cell extract, we substituted an N-terminal epitope antibody for K41233 in the ELISA assay (Fig. 6b, left). Notably, enhanced recognition of mutated Hsp90 proteins by K41233 required that Hsp90 be in its native conformation. When we immunoprecipitated Hsp90 proteins with antibody to Flag, subjected them to denaturing SDS-PAGE and blotted with K41233, we saw no differential sensitivity (Fig. 6c). Taken together, these data support our hypothesis that mutation of the IxL motif in  $\beta$ -strand 8 alters accessibility of the charged linker.

### $\beta$ -strand 8 mutation disrupts N-domain structure

Amide hydrogen exchange measurements can be used to query structural changes of solution-phase proteins, because solvent-exposed regions will exchange hydrogen atoms at a faster rate than will highly structured or buried regions<sup>33,34</sup>. As an approach to understanding the impact of  $\beta$ -strand 8 mutation on Hsp90 conformation, we sought to obtain more information on the consequences of  $\beta$ -strand 8 mutation for the structural integrity of Hsp90. Therefore, we assessed rates of amide hydrogen exchange for both yeast wild-type and I205A Hsp90 proteins, and we compared the solvent accessibility of a series of peptides comprising the various domains of each protein. First, we found that the I205A mutant incorporated more deuterons than did wild-type Hsp90 (Fig. 7a), suggesting that certain structural elements were more solvent exposed in the mutant protein. Because we observed no difference in exchange rates for peptides covering other regions of the protein (data not shown), we looked more closely at deuterium incorporation into a series of peptides derived from the N domain. In this region, we found greater solvent accessibility for Hsp90 I205A (compared to wild type) in peptides encompassing both  $\beta$ -strand 8 and an adjacent  $\alpha$  helix (Fig. 7b,c). ATP further accentuated differential deuterium incorporation between mutant and wild-type Hsp90 in the peptide encompassing  $\beta$ -strand 8 (201–207), likely reflecting the lack of ATP-induced stabilization of this region in the mutant protein. Crystal structures of yeast Hsp90 support the existence of stabilizing hydrophobic interactions between  $\beta$ -strand 8 with the adjacent helix region comprising amino acids 187–197 (Fig. 8). Substitution of the hydrophobic amino acid isoleucine with the much less hydrophobic

amino acid alanine would therefore result in destabilization of both the helix and the  $\beta$ -strand, leading to increased solvent accessibility and deuterium incorporation in this region. Consistent with the impact of linker truncation on trypsin sensitivity of Hsp90 I218A, analysis of deuterium incorporation by linker-truncated Hsp90 I205A (L-I205A in Fig. 7b) revealed that linker truncation stabilized  $\beta$ -strand 8 in the presence and absence of ATP, thus partially compensating for the reduced stability in regions 186–200 ( $\alpha$  helix) and 201–207 ( $\beta$ -strand 8) induced by I205A mutation. Further, linker truncation in the absence of I205A mutation markedly stabilized  $\beta$ -strand 8 in the presence and absence of ATP (Fig. 7b), providing direct evidence of the impact of the charged linker on conformational dynamics of the Hsp90 N domain.

## DISCUSSION

This study was initially undertaken to identify surface-exposed motifs in Hsp90 that are necessary for the chaperone's nonclassical secretion. After mutagenizing several surface-exposed amino acid residues, we identified a highly conserved Ile218 and Leu220 in  $\beta$ -strand 8 of the N domain of human Hsp90 whose mutation to alanine, either separately or together, markedly reduced Hsp90 secretion. Both amide hydrogen exchange data and trypsin sensitivity measurements suggest that a single mutation in  $\beta$ -strand 8 (I205A in yeast, equivalent to I218A in human Hsp90) does not affect the global structural integrity of Hsp90, but instead only affects discrete regions of the N domain comprising  $\beta$ -strand 8 itself and an adjacent  $\alpha$  helix. These findings support our hypothesis that reduced secretion is a direct result of the altered structural integrity of this region of the N domain adjoining the charged linker.

Unexpectedly, we found that locally increased conformational flexibility created by a  $\beta$ -strand 8 mutation greatly altered the chaperone activity of Hsp90 while shifting its conformational equilibrium to a more open state. Steady-state interaction with several kinase and steroid receptor clients was reduced, and the I218A L220A mutant was unable to promote reconstitution of CHK1 kinase activity *in vitro*. Specific co-chaperone interactions were also altered, fitting a model in which  $\beta$ -strand 8-mutated Hsp90 exists primarily in an open conformation (for example, N domains not dimerized) with low affinity for client proteins. Consistent with this model, the ATPase activity of  $\beta$ -strand 8-mutated Hsp90 (both yeast and human proteins) was less than half that of wild type, and its AMPPNP-stabilized N-terminal dimerization was significantly lower than that of wild-type Hsp90. This model is further supported by real-time FRET analysis of Hsp90 domain-domain interactions in solution.

Neither yeast nor human  $\beta$ -strand 8 mutants were able to support yeast viability. Notably, neither loss of ATPase activity nor inability to form N-terminal dimers directly contributed to the reduced secretion of  $\beta$ -strand 8 mutants, because other well-characterized Hsp90 mutations that result in similar defects failed to affect secretion. These findings are consistent with a recent report that neither ATP binding nor ATPase activity are necessary for the extracellular activity of Hsp90 (ref. 19). From these data, we conclude that alteration of the structural integrity in the region of the N domain adjacent to the charged linker affects



secretory capability independently from the other parameters of chaperone function that we examined.

Little is known about the importance of  $\beta$ -strand 8 and the surrounding region for Hsp90 function. Amide hydrogen-deuterium exchange measurements of human Hsp90 have suggested that this region becomes less accessible to solvent upon binding of inhibitor ligand to the N domain<sup>7</sup>. Recent data obtained for the bacterial Hsp90 ortholog HtpG show that the helix adjacent to  $\beta$ -strand 8 is greatly stabilized upon addition of ATP, presumably as a result of conformational changes that create novel contacts between the N and M domain<sup>20</sup>. Supporting this suggestion, a recent crystallographic study found that, in the nucleotide-bound closed conformation of Hsp90, the N and M domains interact via an anti-parallel  $\beta$ -strand involving  $\beta$ -strand 8 and residues from the M domain<sup>21</sup>.

These observations focused our attention on the possible contribution of the charged linker to the impact of  $\beta$ -strand 8 mutation on Hsp90 function. Given its disordered nature, this region of the protein has proven difficult to visualize structurally, but our study provides five pieces of data implicating the charged linker's contribution to the effects of  $\beta$ -strand 8 mutation on Hsp90. First, mutated Hsp90 demonstrated increased protease sensitivity at a previously identified site at the junction of the linker and M domain. Mutation of both hydrophobic residues in  $\beta$ -strand 8 also resulted in increased trypsin sensitivity at a C-terminal location, suggesting a more global impact on Hsp90 conformation. Notably, truncation of the charged linker prevented propagation of this conformational change. Second, recognition of Hsp90 in solution by a charged linker-directed antibody was markedly enhanced by  $\beta$ -strand 8 mutation. Third, analysis of deuterium incorporation in wild-type and linker-truncated Hsp90 mutants revealed that charged-linker truncation partially reverses destabilization within the N domain induced by  $\beta$ -strand 8 mutation. Notably, even in the absence of  $\beta$ -strand 8 mutation, linker truncation results in significant stabilization of  $\beta$ -strand 8, in the presence and absence of ATP. Fourth, the secretory capability of these mutants was partially recovered following charged-linker truncation. Fifth, and most remarkably, truncation of the charged linker reversed lethality, and restored chaperone function and full ATPase activity to  $\beta$ -strand 8-mutated Hsp90.

Amide hydrogen exchange data confirm a role for localized ATP-induced conformational changes in the region of  $\beta$ -strand 8 in initiating the series of conformational changes that comprise the Hsp90 chaperone cycle. Removal of even one hydrophobic contact (I205A) in the  $\beta$ -strand destabilized both the  $\beta$ -strand and the adjacent helix. Based on FRET analysis of domain interactions, our data suggest that destabilization of this helix prevents repositioning of N and M domains upon ATP binding. Our findings are consistent with a direct impact of  $\beta$ -strand 8 mutation on the conformational dynamics of Hsp90 necessary to convert the chaperone from an open to a closed state. Given that charged-linker truncation can reverse the negative impact of  $\beta$ -strand 8 mutation on Hsp90 function, and that linker truncation itself results in  $\beta$ -strand 8 stabilization in wild-type Hsp90, it follows that the deleterious functional consequences resulting from weakened hydrophobic contacts in this region of the N domain require the conformational freedom supplied by the presence of the charged linker.

## METHODS

Methods and any associated references are available in the online version of the paper at <http://www.nature.com/nsmb/>.

## ONLINE METHODS

### Strains and plasmids.

We used the *S. cerevisiae* strain PP30 (*a, trp1-289, leu2-3,112, his3-200, ura3-52, ade2-101oc, lys2-801am, hsc82KANMX4, hsp-82KANMX4*) as the host strain for expression of *HSP82* mutant alleles as previously described<sup>26</sup>. Its essential Hsp90 function is provided by the *HSC82* gene of the plasmid pHSC82. We introduced the I205A, Q206A and L207A point mutants, as well as the charged-linker truncation mutant (with residues 214–261 deleted), into the *HSP82* gene of the plasmid pHSP82, which we transformed into PP30 yeast. To generate yeast expressing only *HSP82* or its mutants, we cured pHSC82 by streaking the transformants on drop-out medium without leucine, but containing 5-FOA (0.1% (w/v)). pHsp82 is His6 tagged at the N-terminus domain; however, this does not interfere with Hsp82 chaperone function. We subcloned Hsp82 point and deletion mutants into the bacterial plasmid pRSETA as previously described<sup>26</sup>.

We constructed the plasmids pcDNA3-Flag-HSP90 $\alpha$  and pcDNA3-ERBB2 as described previously<sup>35–37</sup>. The AR expression plasmid was a kind gift from D. Smith (Mayo Clinic). We generated all human and yeast Hsp90 mutants using the protocol of the QuikChange site-directed mutagenesis kit (Stratagene). We confirmed Hsp82 and HSP90 $\alpha$  mutant constructs by sequencing the entire DNA.

### Growth conditions.

We grew yeast cells on YPD (2% (w/v) Bacto peptone, 1% (w/v) yeast extract, 2% (w/v) glucose), or on YPGal (YPD with 2% (w/v) galactose, 20 mg l<sup>-1</sup> adenine). Selective growth was on dropout 2% (w/v) glucose (DO) medium supplemented with appropriate amino acids.

We cultured COS7 cells (American Type Culture Collection) in a temperature-controlled incubator (37 °C and 5% CO<sub>2</sub>) in DMEM medium supplemented with 10% (v/v) FBS, 10 mM HEPES (pH 7.0), 2 mM glutamine, 1 mM sodium pyruvate and nonessential amino acids (Biosource/Invitrogen). We transiently transfected COS7 cells using FuGene6 (Roche Applied Science), following the manufacturer's instructions.

### *In vivo* activation of v-Src.

*v-SRC* is under control of the *GALI* promoter. We analyzed its induction and activation as described previously<sup>38</sup>, with the exception that we grew yeast cells on 2% (w/v) glucose in order to repress the *GALI* promoter. We also spotted cells onto YPD or YPGal-2% (w/v) agar. We detected v-Src protein levels with EC10 mouse antibody and v-Src activity with 4G10 mouse anti-phosphotyrosine antibody (both from Millipore).

### ELISA, immunoprecipitation, immunoblotting and trypsin proteolysis.

We transfected and lysed COS7 cells as described previously<sup>35</sup>. To detect secreted HSP90 proteins by ELISA, we collected, clarified and concentrated conditioned medium using an Amicon Ultra-50k centrifugal filter device (Millipore). We incubated samples for 1 h at room temperature (22 °C) with anti-Flag antibody (Sigma), and further incubated them with anti-HSP90 antibody (HSP90 $\alpha$  antibody from Affinity Bioreagents or charged linker-reactive antibody K41233 from Cosmo Bio) and horseradish peroxidase-labeled anti-rabbit IgG (Amersham). We visualized the reaction by addition of the substrate 3,3',5,5'-tetramethylbenzidine and stop reagent (Sigma), and we measured the absorbance at 450 nm in an ELISA plate reader (Model ELx808IU, Bio-TEK instruments). We used total amount of cellular HSP90 to normalize the amount of secreted HSP90, and we expressed the data as relative to wild-type HSP90.

For immunoprecipitations, we incubated cell lysates for 2 h at 4 °C with anti-Flag antibody-conjugated beads (Sigma) or with either anti-FKBP52 (Stressgen) or anti-p60<sup>Hop</sup> (Stressgen) antibody and protein G-agarose. We identified co-immunoprecipitated proteins by immunoblotting with indicated antibodies recognizing Flag (Affinity Bioreagents), HA (Covance), ERBB2 (Santa Cruz), CDK4 (Santa Cruz), RAF1 (Santa Cruz), GR (Santa Cruz), AR (Santa Cruz), p60<sup>Hop</sup> (Cell Signaling), HSP70 (Stressgen), p50<sup>Cdc37</sup> (Neomarkers), p23 (Affinity Bioreagents), AHA1 (Rockland), MYC (Sigma), Tetra-His (Qiagen) or MPK1 ( $\gamma$ -244; Santa Cruz).

For trypsin partial proteolysis, we incubated immunoprecipitates with 500 mM NaCl. We digested equal amounts of Hsp90 with two concentrations (7 and 14  $\mu\text{g ml}^{-1}$ ) of tosyl phenylalanyl chloromethylketone (TCPK)-treated trypsin (Worthington). We incubated the reactions on ice for 6 min and detected fragments by immunoblotting with N-terminal anti-HSP90 antibody (Affinity Bioreagents).

### CHK1 kinase assay.

We determined CHK1 activity as described previously<sup>22</sup>. Briefly, we incubated bead-bound CHK1 with [ $\gamma$ -<sup>32</sup>P]ATP, the CHK1 substrate GST-CDC25C (residues 200–256), and HSP90 proteins (as indicated on figures) at 30 °C for 10 min. Reactions were separated by SDS-PAGE and transferred to Immobilon-P membrane (Millipore). We detected and quantified membrane-bound radiolabeled proteins using a Storm 840 PhosphorImager (Amersham Biosciences).

### ATPase activity and cross-linking experiments.

We determined ATPase activities using a method previously described<sup>26,39</sup>. This is an enzyme-coupled assay using typically 2  $\mu\text{M}$  yeast Hsp90 and 20  $\mu\text{M}$  human Hsp90. All activities are averages of three or more separate measurements and error bars represent s.d. We assessed Hsp90 cross-linking using a method previously described<sup>24</sup>. Briefly, we treated reaction tubes containing protein at 0.5  $\text{mg ml}^{-1}$ , 100 mM HEPES, pH 8.0, 150 mM KCl, 6 mM  $\text{MgCl}_2$ , and either 5 mM ADP or AMPPNP with dimethyl superimide at a concentration of 1.7 mM for 60 min at room temperature.

### Amide hydrogen exchange.

We performed hydrogen exchange experiments as described earlier<sup>40</sup>. We initiated amide hydrogen exchange by a 20-fold dilution of 200 pmol wild-type or mutant Hsp82 into D<sub>2</sub>O containing 25 mM HEPES, pH 7.4, 50 mM KCl, and 5 mM MgCl<sub>2</sub> at 30 °C. After various time points (10 s–90 min), we quenched the exchange reaction by decreasing the temperature to 0 °C and the pH with ice-cold quench buffer (400 mM KH<sub>2</sub>PO<sub>4</sub>/H<sub>3</sub>PO<sub>4</sub>, pH 2.2). We directly injected quenched samples into an HPLC-MS setup as described<sup>40,41</sup>. We generated peptic peptides online by including a column with immobilized pepsin into the HPLC setup. We used a fully deuterated Hsp82 sample as control for back exchange during the desalting and MS analysis. When indicated, proteins were preincubated with excess ATP for 10 min at 30 °C. We performed data acquisition and analysis as described<sup>41</sup>.

### FRET analysis.

We created cysteine point mutations in the I205A mutant using the QuickChange Multi Site-Directed Mutagenesis Kit (Stratagene). We designed the primers using the program provided on the Stratagene website. We carried out protein expression and purification as described<sup>42</sup>. We labeled the wild-type and I205A yeast Hsp90 cysteine mutants with the fluorescence molecules (AttoTec, Siegen) by maleimide chemistry, as described previously<sup>6</sup>. We carried out all single-molecule fluorescence measurements in a custom-built prism-type total internal reflection fluorescence (TIRF) microscope as described<sup>6</sup>.

### Supplementary Material

Refer to Web version on PubMed Central for supplementary material.

### ACKNOWLEDGMENTS

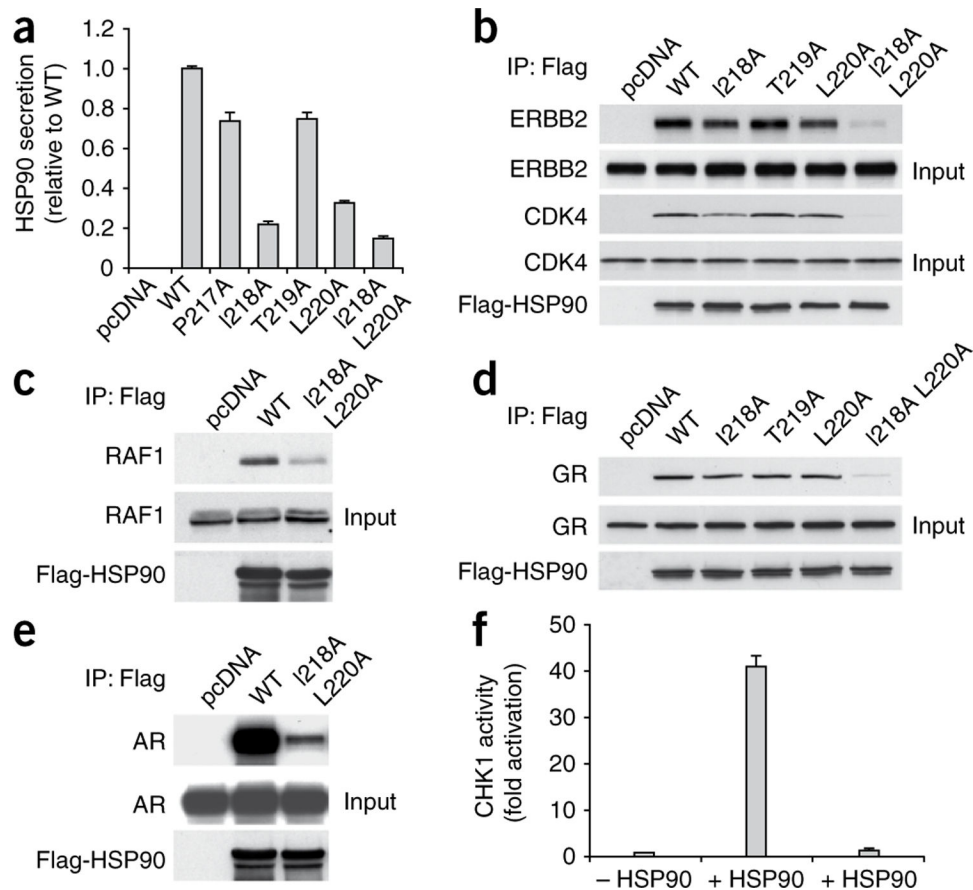
We are indebted to K. Beebe for comments on the manuscript. This work is supported by US National Cancer Institute intramural research funds. S.T. is partially supported by a fellowship from the Japanese Society of the Promotion of Science.

### References

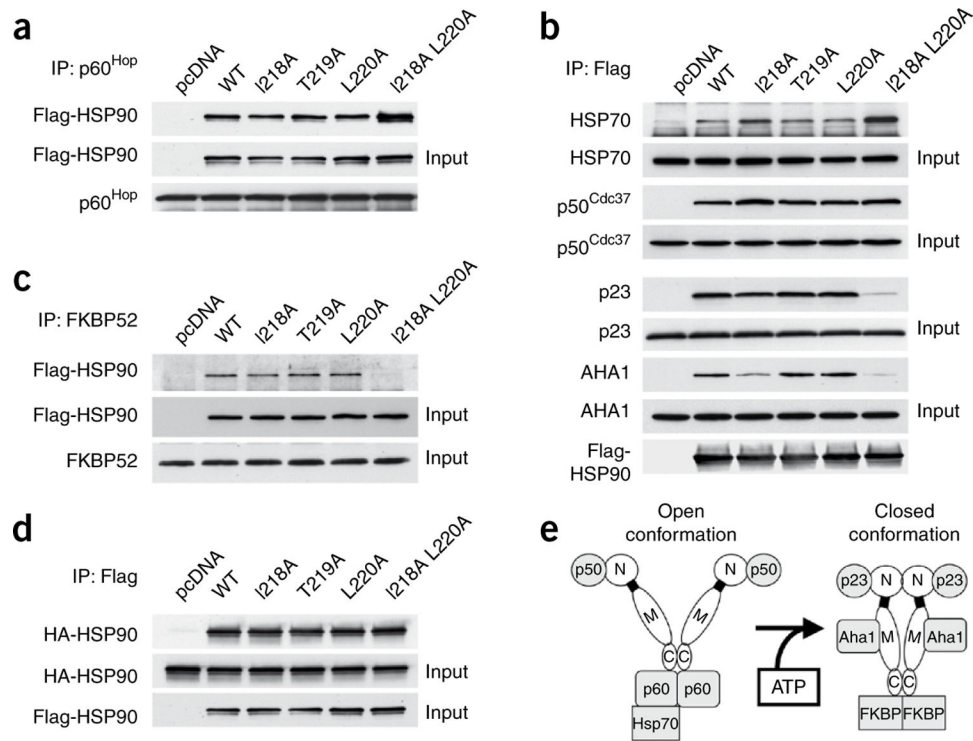
1. Neckers LHsp90 inhibitors as novel cancer chemotherapeutic agents. *Trends Mol. Med*8, S55–S61 (2002). [PubMed: 11927289]
2. Pearl LH & Prodromou C Structure and mechanism of the Hsp90 molecular chaperone machinery. *Annu. Rev. Biochem* 75, 271–294 (2006). [PubMed: 16756493]
3. Wandinger SK, Richter K & Buchner J The Hsp90 chaperone machinery. *J. Biol. Chem* 283, 18473–18477 (2008). [PubMed: 18442971]
4. Picard DHeat-shock protein 90, a chaperone for folding and regulation. *Cell. Mol. Life Sci*59, 1640–1648 (2002). [PubMed: 12475174]
5. Blagg BS & Kerr TD Hsp90 inhibitors: small molecules that transform the Hsp90 protein folding machinery into a catalyst for protein degradation. *Med. Res. Rev* 26, 310–338 (2006). [PubMed: 16385472]
6. Hessling M, Richter K & Buchner J Dissection of the ATP-induced conformational cycle of the molecular chaperone Hsp90. *Nat. Struct. Mol. Biol* 16, 287–293 (2009). [PubMed: 19234467]
7. Phillips JJet al. Conformational dynamics of the molecular chaperone Hsp90 in complexes with a co-chaperone and anticancer drugs. *J. Mol. Biol*372, 1189–1203 (2007). [PubMed: 17764690]

8. Bron Pet al. Apo-Hsp90 coexists in two open conformational states in solution. *Biol. Cell* 100, 413–425 (2008). [PubMed: 18215117]
9. Shiau AK, Harris SF, Southworth DR & Agard DA Structural analysis of *E. coli* hsp90 reveals dramatic nucleotide-dependent conformational rearrangements. *Cell* 127, 329–340 (2006). [PubMed: 17055434]
10. Southworth DR & Agard DA Species-dependent ensembles of conserved conformational states define the Hsp90 chaperone ATPase cycle. *Mol. Cell* 32, 631–640 (2008). [PubMed: 19061638]
11. Mickler M, Hessling M, Ratzke C, Buchner J & Hugel T The large conformational changes of Hsp90 are only weakly coupled to ATP hydrolysis. *Nat. Struct. Mol. Biol* 16, 281–286 (2009). [PubMed: 19234469]
12. Vaughan CK et al. Structure of an Hsp90-Cdc37-Cdk4 complex. *Mol. Cell* 23, 697–707 (2006). [PubMed: 16949366]
13. Felts SJ et al. The hsp90-related protein TRAP1 is a mitochondrial protein with distinct functional properties. *J. Biol. Chem* 275, 3305–3312 (2000). [PubMed: 10652318]
14. Scheibel Tet al. The charged region of Hsp90 modulates the function of the N-terminal domain. *Proc. Natl. Acad. Sci. USA* 96, 1297–1302 (1999). [PubMed: 9990018]
15. Louvion JF, Warth R & Picard D Two eukaryote-specific regions of Hsp82 are dispensable for its viability and signal transduction functions in yeast. *Proc. Natl. Acad. Sci. USA* 93, 13937–13942 (1996). [PubMed: 8943039]
16. Tsutsumi S & Neckers L Extracellular heat shock protein 90: a role for a molecular chaperone in cell motility and cancer metastasis. *Cancer Sci* 98, 1536–1539 (2007). [PubMed: 17645779]
17. Binder RJ, Vatner R & Srivastava P The heat-shock protein receptors: some answers and more questions. *Tissue Antigens* 64, 442–451 (2004). [PubMed: 15361121]
18. Clayton A, Turkes A, Navabi H, Mason MD & Tabi Z Induction of heat shock proteins in B-cell exosomes. *J. Cell Sci* 118, 3631–3638 (2005). [PubMed: 16046478]
19. Cheng CF et al. Transforming growth factor alpha (TGF $\alpha$ )-stimulated secretion of HSP90 $\alpha$ : using the receptor LRP-1/CD91 to promote human skin cell migration against a TGF $\beta$ -rich environment during wound healing. *Mol. Cell. Biol* 28, 3344–3358 (2008). [PubMed: 18332123]
20. Graf C, Stankiewicz M, Kramer G & Mayer MP Spatially and kinetically resolved changes in the conformational dynamics of the Hsp90 chaperone machine. *EMBO J* 28, 602–613 (2009). [PubMed: 19165152]
21. Ali MM et al. Crystal structure of an Hsp90-nucleotide-p23/Sba1 closed chaperone complex. *Nature* 440, 1013–1017 (2006). [PubMed: 16625188]
22. Arlander SJ et al. Chaperoning checkpoint kinase 1 (Chk1), an Hsp90 client, with purified chaperones. *J. Biol. Chem* 281, 2989–2998 (2006). [PubMed: 16330544]
23. Pratt WB & Toft DO Regulation of signaling protein function and trafficking by the hsp90/hsp70-based chaperone machinery. *Exp. Biol. Med. (Maywood)* 228, 111–133 (2003). [PubMed: 12563018]
24. Prodromou C et al. The ATPase cycle of Hsp90 drives a molecular ‘clamp’ via transient dimerization of the N-terminal domains. *EMBO J* 19, 4383–4392 (2000). [PubMed: 10944121]
25. Millson SH et al. Expressed as the sole Hsp90 of yeast, the  $\alpha$  and  $\beta$  isoforms of human Hsp90 differ with regard to their capacities for activation of certain client proteins, whereas only Hsp90 $\beta$  generates sensitivity to the Hsp90 inhibitor radicicol. *FEBS J* 274, 4453–4463 (2007). [PubMed: 17681020]
26. Panaretou B et al. ATP binding and hydrolysis are essential to the function of the Hsp90 molecular chaperone in vivo. *EMBO J* 17, 4829–4836 (1998). [PubMed: 9707442]
27. Panaretou B et al. The Hsp90 of *Candida albicans* can confer Hsp90 functions in *Saccharomyces cerevisiae*: a potential model for the processes that generate immunogenic fragments of this molecular chaperone in *C. albicans* infections. *Microbiology* 145, 3455–3463 (1999). [PubMed: 10627043]
28. Grenert JP, Johnson BD & Toft DO The importance of ATP binding and hydrolysis by hsp90 in formation and function of protein heterocomplexes. *J. Biol. Chem* 274, 17525–17533 (1999). [PubMed: 10364185]

29. Nemoto T, Sato N, Iwanari H, Yamashita H & Takagi T Domain structures and immunogenic regions of the 90-kDa heat-shock protein (HSP90). Probing with a library of anti-HSP90 monoclonal antibodies and limited proteolysis. *J. Biol. Chem* 272, 26179–26187 (1997). [PubMed: 9334185]
30. Czar MJ et al. Characterization of the protein-protein interactions determining the heat shock protein (hsp90.hsp70.hsp56) heterocomplex. *J. Biol. Chem* 269, 11155–11161 (1994). [PubMed: 8157642]
31. Hartson SD et al. p50(cdc37) is a nonexclusive Hsp90 cohort which participates intimately in Hsp90-mediated folding of immature kinase molecules. *Biochemistry* 39, 7631–7644 (2000). [PubMed: 10858314]
32. Yun BG, Huang W, Leach N, Hartson SD & Matts RL Novobiocin induces a distinct conformation of Hsp90 and alters Hsp90-cochaperone-client interactions. *Biochemistry* 43, 8217–8229 (2004). [PubMed: 15209518]
33. Tsutsui Y & Winrod PL Hydrogen/deuterium exchange-mass spectrometry: a powerful tool for probing protein structure, dynamics and interactions. *Curr. Med. Chem* 14, 2344–2358 (2007). [PubMed: 17896983]
34. Lanman J & Prevelige PE Jr. High-sensitivity mass spectrometry for imaging subunit interactions: hydrogen/deuterium exchange. *Curr. Opin. Struct. Biol* 14, 181–188 (2004). [PubMed: 15093832]
35. Scroggins BT et al. An acetylation site in the middle domain of Hsp90 regulates chaperone function. *Mol. Cell* 25, 151–159 (2007). [PubMed: 17218278]
36. Tzahar E et al. A hierarchical network of interreceptor interactions determines signal transduction by Neu differentiation factor/neuregulin and epidermal growth factor. *Mol. Cell Biol* 16, 5276–5287 (1996). [PubMed: 8816440]
37. Xu W et al. Chaperone-dependent E3 ubiquitin ligase CHIP mediates a degradative pathway for c-ErbB2/Neu. *Proc. Natl. Acad. Sci. USA* 99, 12847–12852 (2002). [PubMed: 12239347]
38. Panaretou B et al. Activation of the ATPase activity of hsp90 by the stress-regulated cochaperone hsc70. *Mol. Cell* 10, 1307–1318 (2002). [PubMed: 12504007]
39. Prodromou C et al. Regulation of Hsp90 ATPase activity by tetratricopeptide repeat (TPR)-domain co-chaperones. *EMBO J* 18, 754–762 (1999). [PubMed: 9927435]
40. Rist W, Jorgensen TJ, Roepstorff P, Bukau B & Mayer MP Mapping temperature-induced conformational changes in the *Escherichia coli* heat shock transcription factor sigma 32 by amide hydrogen exchange. *J. Biol. Chem* 278, 51415–51421 (2003). [PubMed: 14504287]
41. Rist W, Graf C, Bukau B & Mayer MP Amide hydrogen exchange reveals conformational changes in hsp70 chaperones important for allosteric regulation. *J. Biol. Chem* 281, 16493–16501 (2006). [PubMed: 16613854]
42. Richter K, Muschler P, Hainzl O & Buchner J Coordinated ATP hydrolysis by the Hsp90 dimer. *J. Biol. Chem* 276, 33689–33696 (2001). [PubMed: 11441008]

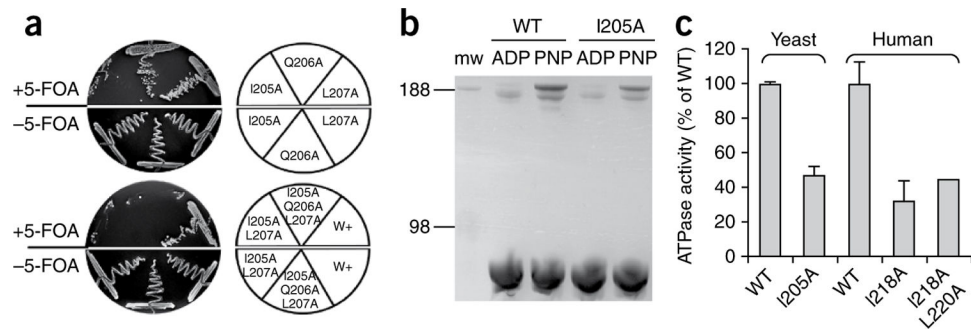
**Figure 1.**

Identification of Ile218 and Leu220 as important for function of human HSP90 $\alpha$ . (a) COS7 cells were transfected with empty vector (pcDNA) or the indicated Flag-HSP90 constructs. After incubation, conditioned medium was collected and secreted HSP90 protein was detected by ELISA. (b–e) COS7 cells were transfected with empty vector (pcDNA) or the indicated Flag-HSP90 constructs (b–e) together with ERBB2 (b), RAF1 (c), GR (d) or AR (e). After incubation, cells were lysed and proteins were immunoprecipitated (IP) by Flag antibody–conjugated agarose and separated by SDS-PAGE. Indicated co-precipitating proteins were detected by immunoblotting. (f) Purified GST-CHK1(1–265) bound to glutathione (GSH)-agarose was incubated with (+Hsp90, middle) or without (–Hsp90, left) purified wild-type (WT) Hsp90 protein or with I218A L220A Hsp90 protein (right) together with HSP70, YDJ, p50<sup>Cdc37</sup>, p60<sup>Hop</sup>, p23 and CK2 (ref. 22). Radiolabeled proteins were imaged and quantified by phosphorimager. Fold CHK1 activation is displayed, and error bars represent s.d. from the mean calculated from three experiments.

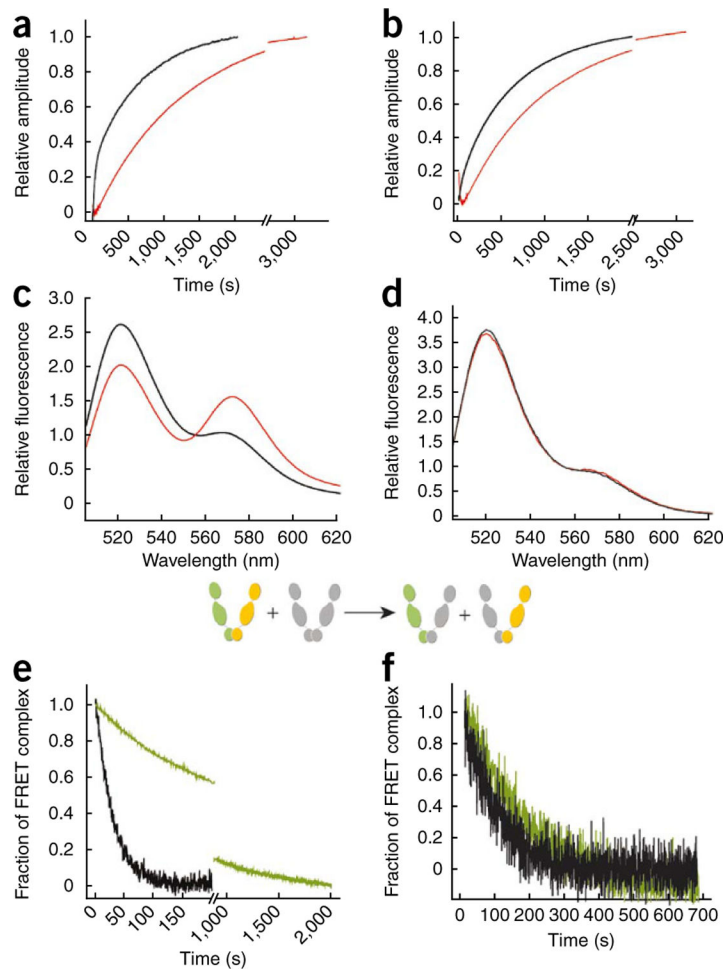


**Figure 2.** Mutation of  $\beta$ -strand 8 attenuates co-chaperone interaction. **(a–d)** COS7 cells were transfected with empty vector (pcDNA) or the indicated Flag-HSP90 constructs. Cells were lysed and proteins were immunoprecipitated (IP) by p60<sup>Hop</sup> antibody **(a)**, by Flag antibody–conjugated agarose **(b,d)** or by FKBP52 antibody **(c)** and then separated by SDS-PAGE. Indicated co-precipitating proteins were detected by immunoblotting. WT, wild type. **(e)** Schematic model for open and closed HSP90 conformation. HSP90 (N, N domain; bold line, charged linker; M, middle domain; C, C domain) binds to p60<sup>Hop</sup> (p60), HSP70 and p50<sup>Cdc37</sup> (p50) in open conformation, and binds to FKBP52 (FKBP), p23 and AHA1 in closed conformation.



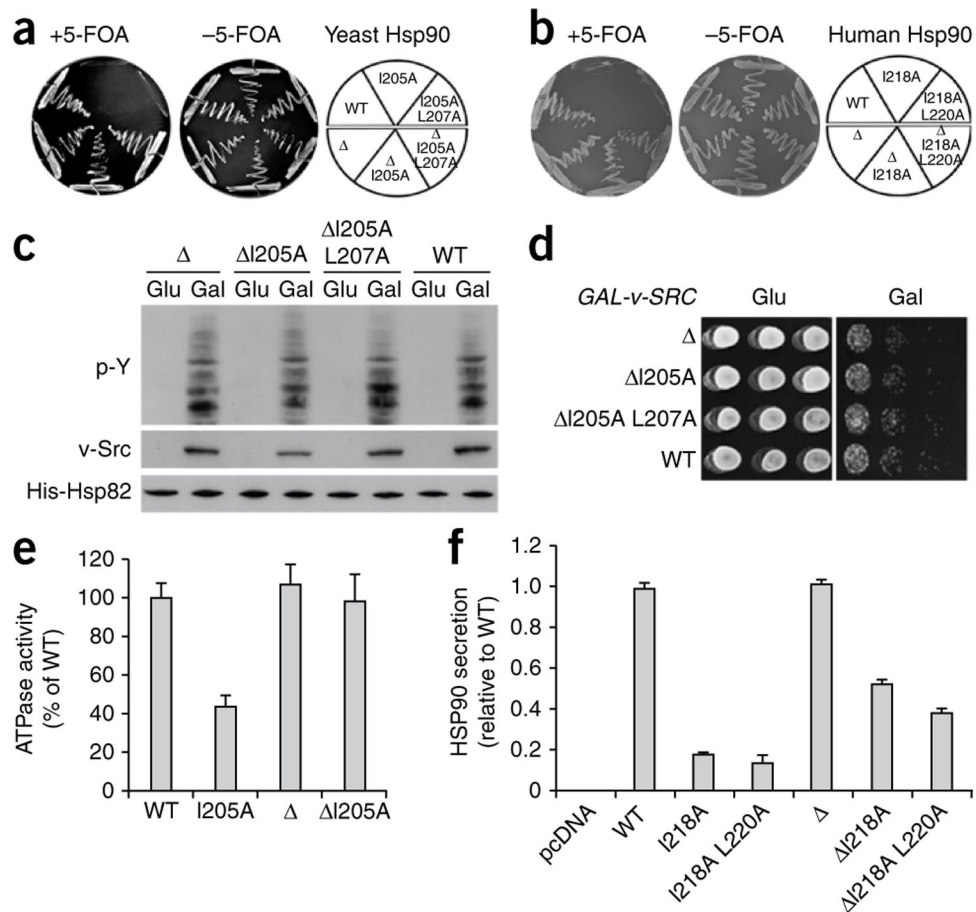


**Figure 3.** Mutation of  $\beta$ -strand 8 attenuates nucleotide-dependent chaperone function. **(a)** A *S. cerevisiae* strain deleted for both genomic copies of yeast *HSP90* but carrying both wild-type (W+) yeast *HSP82* (on a *URA3*-marked plasmid) and yeast *HSP82* constructs. Cells were grown on synthetic defined medium without tryptophan (SD –TRP) plates either with or without 5-FOA at 25 °C for 5 d. **(b)** Polyacrylamide gel of wild-type and mutant I205A Hsp82 proteins cross-linked with dimethyl superimide in the presence of ADP or AMPPNP (PNP); mw: molecular weight (kDa). **(c)** ATPase activities of wild-type and indicated mutant Hsp90 proteins. Error bars represent s.d. from the mean.

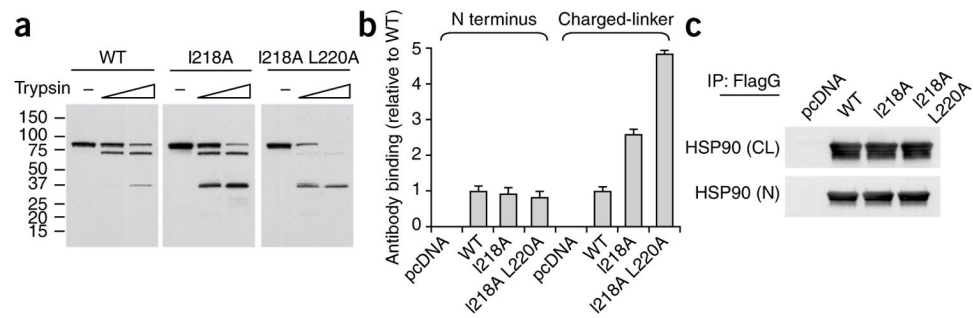


**Figure 4.**

Mutation of  $\beta$ -strand 8 inhibits ATP-induced Hsp90 conformational dynamics. ATP- $\gamma$ S-induced kinetics of conformational changes in Hsp90 were measured by FRET analysis after rapid mixing. (a) 200 nM wild-type yeast Hsp90 (black traces) or yeast Hsp90 I205A (red traces) proteins were labeled with the fluorescent dyes ATTO488 (donor) and ATTO550 (acceptor) at the S61C substitution in the N domain of the respective protomers<sup>6</sup>. (b) Hsp90 proteins were labeled at S61C in the N domain of one protomer and at Q385C in the M domain of the second protomer<sup>6</sup>. (c) Aha1-induced conformational changes in wild-type yeast Hsp90 were assessed by monitoring FRET efficiencies of Hsp90 S61C labeled with ATTO488 and ATTO550 in the absence (black trace) or in the presence (red trace) of 10  $\mu$ M Aha1. (d) The same experiment as in c was performed using yeast Hsp90 S61C I205A. (e) Aha1-dependent stabilization of the FRET complex between protomers of wild-type Hsp90 was assayed by a chase with unlabeled wild-type Hsp90. This leads to a dissociation of donor- and acceptor-labeled complexes and a decrease in FRET signal (see scheme insert). In the presence of 10  $\mu$ M Aha1, the FRET complex is more resistant to dissociation (green trace) than it is in the absence of Aha1 (black trace). (f) The same experiment as in e but using Hsp90 I205A protein. In this case, Aha1 is unable to stabilize the FRET complex.

**Figure 5.**

Truncation of the charged linker restores function to  $\beta$ -strand 8 Hsp90 mutants. **(a,b)** An *S. cerevisiae* strain with both genomic copies of yeast *HSP90* deleted but carrying both wild-type yeast *HSP82* (on a URA3-marked plasmid) and either yeast *Hsp90* constructs ( : 214–261; **a**) or human *Hsp90* constructs ( : 227–281; **b**). Cells were grown on SD –TRP plates either with or without 5-FOA at 25 °C for 5 d. **(c,d)** v-Src under control of the GAL1 promoter was transformed into the same cells expressing the charged linker–deleted wild-type ( ) and mutant versions, I205A and I205A L207A. Growth of these cells in the presence of glucose (Glu) represses v-Src expression, which is induced with galactose (Gal). *In vitro* v-Src activity and protein expression were detected by immunoblotting **(c)**, and *in vivo* v-Src activity was determined by its effects on cell growth **(d)**, by immunoblotting using antibodies to phosphotyrosine (p-Y) and v-Src, respectively. **(e)** ATPase activities of wild-type and indicated mutant Hsp82 proteins. Data are displayed as mean  $\pm$  s.d. **(f)** COS7 cells were transfected with empty vector (pcDNA) or indicated Flag-Hsp90 constructs ( : 227–281). After incubation, conditioned medium was collected and secreted Hsp90 protein was detected by ELISA. Data are displayed as mean  $\pm$  s.d.

**Figure 6.**

$\beta$ -strand 8 mutation alters the conformational state of the charged linker. **(a–c)** COS7 cells were transfected with indicated Flag-HSP90 constructs. **(a)** Cells were lysed and proteins were immunoprecipitated by Flag antibody–conjugated agarose. Immunoprecipitates were digested with TCPK-treated trypsin and detected by immunoblotting with N-terminal antibody to HSP90. Molecular weight (kDa) is shown on the left. **(b)** Cells were lysed, and reactivity of natively folded HSP90 proteins against N terminus or charged-linker antibody was determined by ELISA. Error bars represent s.d. from the mean. **(c)** Cells were lysed, and reactivity of denatured HSP90 proteins against N-terminal or charged-linker antibody was determined by immunoblotting. CL, charged-linker antibody; N, N-terminus antibody.

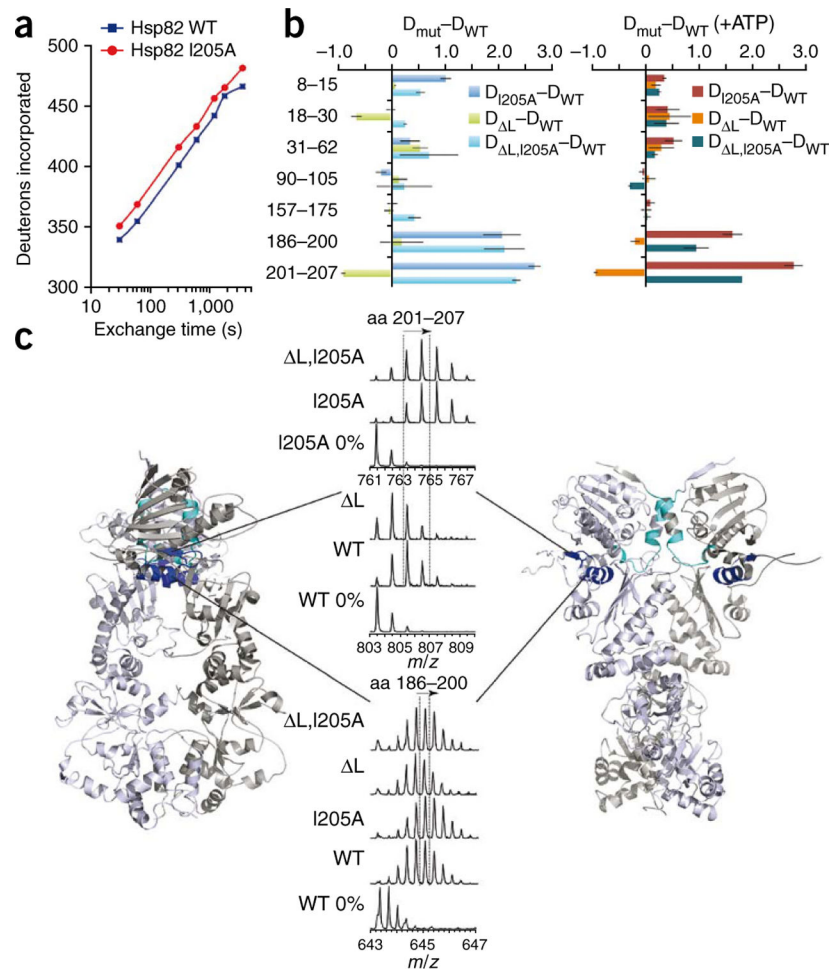


**Figure 7.** Impact of  $\beta$ -strand 8 mutation on deuterium incorporation kinetics of Hsp82. **(a)** Deuterium incorporation over a period of 3,600 s was determined for purified full-length wild-type (blue) or mutant (I205A, red) Hsp82 protein. Data are expressed as number of deuterons incorporated over time. **(b,c)** After incubation with  $D_2O$  for 30 s, proteins were digested with pepsin and analyzed by mass spectrometry. In **b**, deuterium incorporation into mutant Hsp82 proteins minus deuterium incorporation into wild-type Hsp82 protein during a 30-s incubation in  $D_2O$  in the absence (left) or presence (right) of ATP is plotted for selected peptides derived from the N domain of Hsp82. WT: wild-type Hsp82; I205A: I205A Hsp82; L: Hsp82( 214–261); L,I205A: Hsp82( 214–261)-I205A double mutant. Error bars represent the s.e.m. of three independent experiments. Numbers at left indicate Hsp82 residues. **c** shows a representation of Hsp82 (PDB 2CG9 (ref. 21)) in two orientations rotated by  $90^\circ$ , colored according to difference in deuterium incorporation between mutant (I205A) Hsp82 protein and wild-type Hsp82 protein in the presence of ATP. Dark blue, difference of 1.5 deuterons or more; cyan, difference of 0.5 deuterons or less. Dotted lines indicate the centroid of the isotope distribution for the indicated peptic peptides of wild-type and I205A mutant proteins.

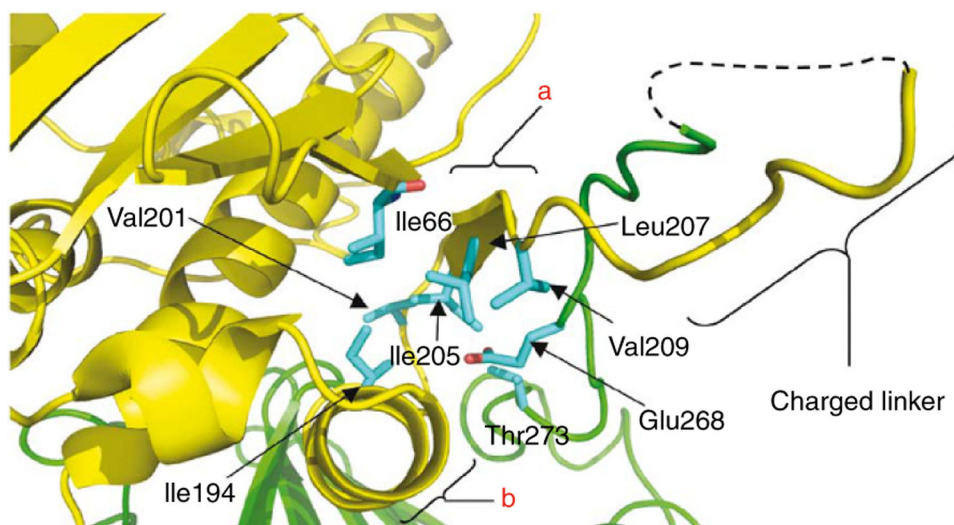


**Figure 8.** Hydrophobic interactions between  $\beta$ -strand 8 and the adjacent  $\alpha$  helix. Cartoon details of the secondary structure including  $\beta$ -strand 8 and the adjacent helix region. (a)  $\beta$ -strand 8. (b)  $\alpha$  helix 9. Charged linker is depicted by a broken line.